

Berezinskii-Kosterlitz-Thouless transition of two-component Bose mixtures with inter-component Josephson coupling

Michikazu Kobayashi¹, Minoru Eto², Muneto Nitta³

¹*Department of Physics, Kyoto University, Oiwake-cho, Kitashirakawa, Sakyo-ku, Kyoto 606-8502, Japan,*

²*Department of Physics, Yamagata University, Kojirakawa-machi 1-4-12, Yamagata 990-8560, Japan,*

³*Department of Physics, and Research and Education Center for Natural Sciences, Keio University, Hiyoshi 4-1-1, Yokohama, Kanagawa 223-8521, Japan*

(Dated: December 16, 2019)

We study the Berezinskii-Kosterlitz-Thouless (BKT) transition of two-component Bose mixtures in two spatial dimensions. When phases of both components are decoupled, half-quantized vortex-antivortex pairs of each component induce two-step BKT transitions. On the other hand, when phases of the both components are synchronized through the inter-component Josephson coupling, two species of vortices of each component are bind to form a molecule, and in this case, we find that there is only one BKT transition by molecule-antimolecule pairs. Our results can be tested by two weakly-connected Bose systems such as two-component ultracold dilute Bose mixtures with the Rabi oscillation, and multiband superconductors.

Phase transitions in two-dimensional systems with a continuous symmetry have long attracted much attentions since the theoretical prediction by Berezinskii, Kosterlitz and Thouless (BKT), providing a topological ordering through the binding of vortex-antivortex pairs [1, 2]. Being different from the conventional thermodynamic transition prohibited by the Coleman-Mermin-Wagner theorem in two-dimensional systems [3–5], the BKT transition exhibits a critical line below the BKT transition temperature, $T \leq T_{\text{BKT}}$, with continuously variable critical exponents and the nonzero helicity modulus (superfluid density) showing discontinuous jump at the BKT transition temperature. The BKT transition has been observed in ⁴He films [6], thin superconductors [7–11], Josephson-junction arrays [12, 13], colloidal crystals [14–16], and ultracold atomic Bose gases [17].

One of important issues of the BKT transition is a relationship between its universality and topological aspects of vortices. In the two-dimensional Bose systems with no internal degree of freedom, circulations of vortices are quantized by $2\pi\hbar/m$ with the particle mass m , giving the universal jump of the superfluid number density $\Delta\rho_s$ at the BKT transition temperature T_{BKT} as

$$\Delta\rho_s = \frac{2mT_{\text{BKT}}}{\pi\hbar^2}. \quad (1)$$

On the other hand, multi-component systems in general allow quantized vortices with fractional circulations, which are studied in superfluid ³He [18–20], p -wave superconductors [18, 21–23], multi-band or multi-component superconductors [24–27], spinor Bose systems [28, 29], multicomponent Bose systems [30–47], exciton-polariton condensates [48, 49], nonlinear optics [50], and color superconductors as quark matter [51]. It has been predicted that the relation (1) is changed for superfluid systems with internal degrees of freedom inducing vortices having fractional circulations [52, 53]. However the existence of an unusual BKT transition is not yet conclusive.

Here we consider a two-dimensional Bose system with two different quantum sublevels. We consider the situation in which two phases in the both sublevels can be synchronized through the Josephson or internal coherent coupling. When the Josephson coupling is switched off, vortices for both components have fractional circulation $\pm 2\pi\alpha_i\hbar/m$ ($i = 1, 2$) with the fractional parameter $\alpha_i \in (0, 1)$ for the i -th component with $\alpha_1 + \alpha_2 = 1$. Under a finite Josephson coupling, on the other hand, a single vortex in each component cannot exist as a stable topological defect. Instead, two vortices in both components are connected by a one-dimensional (sine-Gordon) kink [30, 54] to form a vortex molecule as a stable topological defect having the integer circulation $\pm 2\pi\hbar/m$ [30, 36]. Dynamics of such vortex molecules have been studied in Refs. [45, 46] and vortex lattices have been studied in Refs. [41, 47].

In this Letter, we investigate a possibility of the BKT transition in this system and obtain the following results. When the Josephson coupling is switched off, there are two-step BKT transitions induced by bindings of fractional vortex-antivortex pairs of each component. Both the BKT transition temperatures depend on the fractional parameter α_i . The universal relation is changed to twice of the right-hand-side in (1) only when the two BKT transition temperature are the same with $\alpha_1 = \alpha_2 = 1/2$. The universal relation is, on the other hand, unchanged, which suggests that the fractional circulation is never sufficient condition for the change of the universal relation (1) opposed to previous expectations [52, 53, 55, 56]. When the Josephson coupling is switched on, the BKT transition is induced by bindings of molecule-antimolecule pairs with the normal universal relation (1), while the bindings of vortex-antivortex pairs for each component do not give a phase transition but does two crossovers.

Our results can be tested by two weakly connected ultracold Bose gases or an ultracold Bose mixture with two magnetic hyperfine spin sublevels. For these systems, the

inter-component Josephson coupling can be realized by the energy barrier separating two slices or the Rabi oscillation between two sublevels, respectively. The latter system has also been considered as a toy system simulating the quark confinement in quantum chromodynamics (QCD) [45, 46], thereby our result could give some implications for statistical properties such as a transition between confinement and deconfinement phases. Other candidates are multiband superconductors such as superconducting MgB₂ compounds [57–60] and Iron-based superconductors [61–63]; it is predicted that the first one has less Josephson coupling strength than the second one. Although the above materials have not been completely confirmed as multiband superconductors yet, our results would give some guiding principles.

We start from the Hamiltonian $H = \int d^2x \mathcal{H}$ as

$$\mathcal{H} = \sum_{i=1}^2 \left\{ \frac{\hbar^2}{2m} |\nabla \psi_i|^2 + \frac{g_1}{2} |\psi_i|^4 \right\} + g_2 |\psi_1|^2 |\psi_2|^2 - \frac{q}{2} (\psi_1^* \psi_2 + \psi_2^* \psi_1), \quad (2)$$

for two-dimensional Bose mixtures describing two different quantum sublevels coupled by the Josephson oscillation. Here ψ_i ($i = 1, 2$) is the i -th Bose field with the particle mass m , $g_1 > 0$ is the intra-component interaction strength common for both components, $g_2 > 0$ is the inter-component interaction strength, and $q \geq 0$ is the Josephson (Rabi) coupling strength. Here, we set $g_1 > g_2$ for the miscible ground state. Considering a BKT transition as a phenomenon at finite temperatures, we ignore the quantum fluctuation. We further impose an additional constraint $(1/L^2) \int d^2x |\psi_i|^2 = n_i$ ($i = 1, 2$), where n_i and L are the particle number density for the i -th component and the system size, respectively.

Inserting the uniform ground state $\psi_i = \sqrt{n_i} e^{i\varphi_i}$ with the phase φ_i ($i = 1, 2$) for the i -th component into the Hamiltonian (2), we obtain the energy density

$$\mathcal{E} = \frac{g_1 n^2}{2} - (g_1 - g_2) \tilde{n}^2 - q \tilde{n} \cos \Delta\varphi, \quad (3)$$

where $n = n_1 + n_2$, $\tilde{n} = \sqrt{n_1 n_2}$, and $\Delta\varphi = \varphi_1 - \varphi_2$ are the total number density, the geometric mean density, and the relative phase, respectively. The last term of the right-hand-side in Eq. (3) shows that the zero relative phase $\varphi_1 - \varphi_2 = 0$ is selected for the ground state.

We first consider vortices and interactions between them. For $q = 0$, single vortex states

$$\{\pm 1, 0\} : (\psi_1 \sim \sqrt{n_1} e^{\pm i\phi_0}, \psi_2 \sim \sqrt{n_2}), \quad (4)$$

and

$$\{0, \pm 1\} : (\psi_1 \sim \sqrt{n_1}, \psi_2 \sim \sqrt{n_2} e^{\pm i\phi_0}), \quad (5)$$

are topologically stable, with $\phi_0 \equiv \tan^{-1}(y/x)$. The mass circulation κ of vortices is given by

$$\kappa = \frac{\hbar}{m} \oint d\mathbf{l} \cdot \left(\frac{|\psi_1|^2 \nabla \varphi_1 + |\psi_2|^2 \nabla \varphi_2}{|\psi_1|^2 + |\psi_2|^2} \right), \quad (6)$$

where \mathbf{l} is the vector for the closed path surrounding a vortex. The circulation is $\kappa_1 = \pm 2\pi \alpha_1 \hbar/m$ for vortices $\{\pm 1, 0\}$ and $\kappa_2 = \pm 2\pi \alpha_2 \hbar/m$ for vortices $\{0, \pm 1\}$, where $\alpha_i \equiv n_i/n$ ($i = 1, 2$) is the fractional parameter for i -th component. The interaction between $\{\pm 1, 0\}$ and $\{0, \pm 1\}$ vortices are weaker than logarithm [38], and real time dynamics of them have been studied in Ref. [44].

For $q > 0$, vortices $\{\pm 1, 0\}$ and $\{0, \pm 1\}$ are no more topologically stable. A stable topological defect with nonzero Josephson coupling strength $q > 0$ is a vortex molecule $[1, 1]_{r_0} : \{1, 0\} \stackrel{r_0}{\sim} \{0, 1\}$ or its antimolecule $[-1, -1]_{r_0} : \{-1, 0\} \stackrel{r_0}{\sim} \{0, -1\}$, where $A \stackrel{r_0}{\sim} B$ indicates that two vortices A and B are placed with the distance r_0 . The circulation of the vortex molecule $[1, 1]_{r_0}$ is $\kappa_M = 2\pi \hbar/m$ which is the same as that for a single-component Bose system. The profile of the relative phase $\Delta\varphi$ for a vortex molecule is illustrated in Fig. 1 (a). A kink structure having the relative phase $\Delta\varphi = \pi$ appears and mediate an attractive force between two vortices that is balanced with repulsion [36]. There are two character-

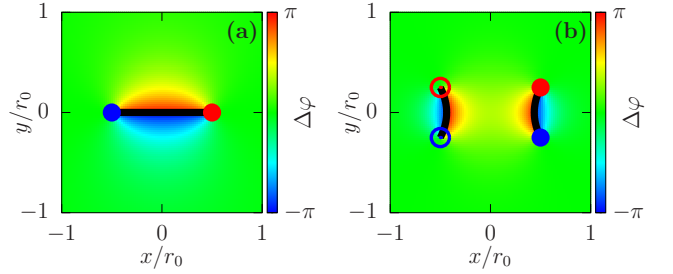


FIG. 1. Profile of the relative phase $\Delta\varphi$ for (a) the vortex molecule $[1, 1]_{r_0}$ and the vortex-molecule pair $[1, 1]_{\delta} \stackrel{r_0}{\sim} [-1, -1]_{\delta}$ with $\delta = 0.5r_0$. Closed (open) red and blue circles represent positions of vortices of $\{1, 0\}$ and $\{0, 1\}$ ($\{-1, 0\}$ and $\{0, -1\}$) respectively. Black solid lines show kinks having the relative phase $\Delta\varphi = \pi$.

istic structures for defect-antidefect pairs. The first is a single component vortex-antivortex pair $\{1, 0\} \stackrel{r_0}{\sim} \{-1, 0\}$ or $\{0, 1\} \stackrel{r_0}{\sim} \{0, -1\}$. The profile of the relative phase for the single-component vortex-antivortex pair is almost same as that shown in Fig. 1 (a), providing the kink between the pair. The second is a molecule-antimolecule pair $[1, 1]_{\delta} \stackrel{r_0}{\sim} [-1, -1]_{\delta}$ with $\delta < r_0$ which is illustrated in Fig. 1 (b).

The leading interaction energy E_{int} between vortices in the large r_0 limit is given as

$$E_{\text{int}}([1, 1]_{r_0}) \sim \varepsilon r_0, \quad (7a)$$

$$E_{\text{int}}(\{1, 0\} \stackrel{r_0}{\sim} \{-1, 0\}) \sim \hbar \kappa_1 n \log(r_0/\xi_1) + \varepsilon r_0, \quad (7b)$$

$$E_{\text{int}}(\{0, 1\} \stackrel{r_0}{\sim} \{0, -1\}) \sim \hbar \kappa_2 n \log(r_0/\xi_2) + \varepsilon r_0, \quad (7c)$$

$$E_{\text{int}}([1, 1]_{\delta} \stackrel{r_0}{\sim} [-1, -1]_{\delta}) \sim \hbar \kappa_M n \log(r_0/\xi), \quad (7d)$$

where $\varepsilon = \gamma \hbar \sqrt{qn\tilde{n}/m}$ is the energy density of the kink per unit length with $\gamma = \mathcal{O}(1)$, ξ_i ($i = 1, 2$) is the vortex core size for the i -th component, and $\xi = \sqrt{\xi_1 \xi_2}$. For $g_1 \gg g_2$, ξ_i is estimated as $\xi_i \sim \hbar/\sqrt{2mgn_i}$. In order to

make the system to exhibit the BKT transition, a pure logarithmic interaction between defect-antidefect pairs is needed. For $q = 0$, single component vortex-antivortex pairs can induce the BKT transition. The BKT transition temperatures depend on the vortex core sizes ξ_i and we expect the two-step BKT transitions for the imbalanced density $n_1 \neq n_2$. For $q > 0$, additional linear terms in Eqs. (7b) and (7c) hinder the BKT transitions by bindings of single component vortex-antivortex pairs connected with kinks. Instead, we expect a new BKT transition by bindings of molecule-antimolecule pairs due to the logarithmic interaction between them in Eq. (7d).

We here show our numerical results by using the standard Metropolis Monte-Carlo sampling for the superfluid number density ρ_s defined as

$$\rho_s = \frac{2m}{\hbar^2} \lim_{\Delta \rightarrow 0} \frac{F(\Delta) - F(0)}{\Delta^2}, \quad (8)$$

where $F(\Delta)$ is the free energy $-T \log Z(\Delta)$ with the partition function $Z(\Delta) = \langle e^{-H/T} \rangle$ under the twisted boundary condition along the x -direction: $\psi_i(x+L, y) = \psi_i(x, y)e^{i\Delta}$. We used $\Delta = 0.01$. Figure 2 shows the temperature dependences of the superfluid density ρ_s with various system sizes L . In Fig. 2 (a), there are strong system size dependence of the superfluid density ρ_s just above two BKT transition temperatures $T_{\text{BKT}1}$ and $T_{\text{BKT}2}$, which can be estimated from the binder ratio (see Appendix). In the thermodynamic limit $L \rightarrow \infty$, the behavior of the superfluid density ρ_s converges to a discrete jump at the BKT transition temperatures. In Fig. 2 (b) for a nonzero Josephson coupling strength, the system size dependence of the superfluid density at around $T_{\text{BKT}} \sim 0.35T_{\text{BKT}}^{(0)}$ disappears, where $T_{\text{BKT}}^{(0)}$ is the BKT transition temperature for the single-component Bose system. The rapidly decreasing structure of the superfluid number density still remains above the temperature $T_{\text{COV}} \sim 0.30T_{\text{BKT}}^{(0)}$. The meaning of the temperature T_{COV} is related to bindings of vortex-antivortex pairs for the first component, as explained later. For the balanced density $n_1/n_2 = 1$, there is only one jump structure of the superfluid density for both zero (Fig. 2 (c)) and nonzero (Fig. 2 (d)) Josephson coupling strengths.

The universal relation in Eq. (1) can be confirmed in Fig. 2: the superfluid density ρ_s and dashed lines for $\rho_s/T = 2m/(\pi\hbar^2)$ intersect at the BKT transition temperature $T = T_{\text{BKT}2}$ in (a) and T_{BKT} in (b) and (d). For $T_{\text{BKT}1}$ in (a), we have the same universal relation, *i.e.*, ρ_s and the dotted line for $(\rho_s - 0.57n)/T = 2m/(\pi\hbar^2)$ intersect at $T = T_{\text{BKT}1}$, where the density $0.57n$ is the estimated superfluid density ρ_s at the temperature just above $T_{\text{BKT}1}$ in the thermodynamic limit $L \rightarrow \infty$. In (c), we have a different universal relation, *i.e.*, ρ_s and dotted line for $\rho_s/T = 4m/(\pi\hbar^2)$ intersect at T_{BKT} , suggesting the twice of the right-hand-side in Eq. (1). The result shown in (a) suggests that the fractional circulation itself does not affect the universal relation, and the change of the universal relation in (c) can be simply understood by considering that the total jump $\Delta\rho_s$

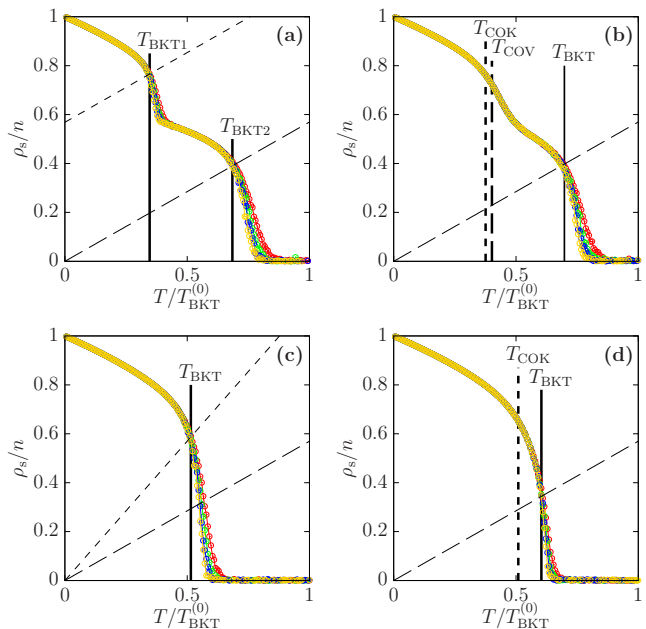


FIG. 2. Superfluid number density ρ_s for (a): $n_1/n_2 = 0.5$ and $q = 0$, (b): $n_1/n_2 = 0.5$ and $q = 0.1g_1n$, (c): $n_1/n_2 = 1$ and $q = 0$, and (d): $n_1/n_2 = 1$ and $q = 0.1gn$ as a function of the temperature $T/T_{\text{BKT}}^{(0)}$, where $T_{\text{BKT}}^{(0)}$ is the BKT transition temperature for the single-component Bose system. The system sizes are $L = 64\xi$ (red lines), $L = 96\xi$ (green lines), $L = 128\xi$ (blue lines), and $L = 160\xi$ (yellow lines). The BKT transition temperatures $T_{\text{BKT}1}$, $T_{\text{BKT}2}$ and T_{BKT} are shown as the thick solid lines. The thin dashed lines in all panels show the relation $\rho_s/T = 2m/(\pi\hbar^2)$. The thin dotted lines in panels (a) and (c) show relations $(\rho_s - 0.57n)/T = 2m/(\pi\hbar^2)$ and $\rho_s/T = 4m/(\pi\hbar^2)$, respectively. The thick dashed line in panel (b) and dotted lines in panels (b) and (d) show the crossover temperatures T_{COV} and T_{COV} , respectively (see Fig. 3).

of the superfluid density is separated into two contributions from the both components. (b) and (d) show that defects inducing the BKT transition change from fractional vortices of each component to vortex molecules and molecule-antimolecule pairs, also supporting the universal relation (1).

We next calculate the thermal average of the number density $\langle \rho_{v1} \rangle$ ($\langle \rho_{v2} \rangle$) of vortex-antivortex pairs for the first (second) component and the length density $\langle \rho_k \rangle$ of kinks. At low temperatures, three densities satisfy the Arrhenius relation $\langle \rho_{v1,v2,k} \rangle \propto e^{-\varepsilon_{v1,v2,k}/T}$. At high temperatures, they deviate from the Arrhenius relation. Figure 3 shows the Arrhenius plots for densities $\rho_{v1,v2,k}$. With the imbalanced density $n_1/n_2 = 0.5$ shown in Fig. 3 (a), the number density $\langle \rho_{v2} \rangle$ (green line) deviates from the Arrhenius relation at the BKT transition temperature T_{BKT} due to unbinding of vortex-antivortex pairs for the second component. The number density ρ_{v1} (red line) and the length density ρ_k (black line), on the other hand, deviate from the Arrhenius relation at

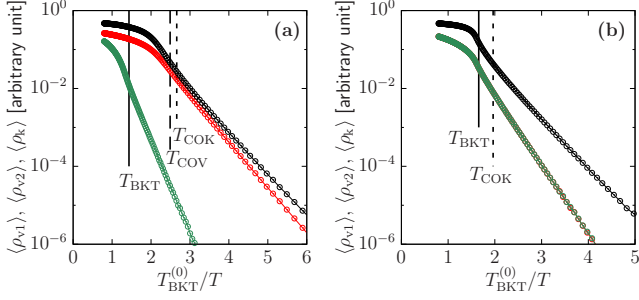


FIG. 3. Arrhenius plots for number densities $\langle\rho_{v1}\rangle$ and $\langle\rho_{v2}\rangle$ of vortex-antivortex pairs for first (red lines) and second (green lines) components, and length density $\langle\rho_k\rangle$ of kinks (black lines) for (a): $n_1/n_2 = 0.5$ and $q = 0.1gn$ and (b): $n_1/n_2 = 1$ and $q = 0.1gn$. The BKT transition temperature T_{BKT} are shown as solid lines. The dashed line in panel (a) and dotted lines in both panels show the crossover temperatures T_{COV} and T_{COK} above which $\langle\rho_{v1}\rangle$ and $\langle\rho_k\rangle$ deviate from the Arrhenius relation, respectively.

lower temperatures $T \simeq 0.40T_{\text{BKT}}^{(0)} = 0.58T_{\text{BKT}} \equiv T_{\text{COV}}$ for ρ_{v1} and $T \simeq 0.38T_{\text{BKT}}^{(0)} = 0.54T_{\text{BKT}} \equiv T_{\text{COK}}$ for ρ_k . The temperature T_{COV} does not induce the BKT transition because of the additional harmonic interaction in Eq. (7b) but shows the crossover for unbinding of vortex-antivortex pairs for the first component with the rapid decrease of the superfluid density ρ_s (see Fig. 2 (b)). At the BKT transition temperature T_{BKT} , some unbounded vortex-antivortex pairs for the first component couple to those for the second component and form molecule-antimolecule pairs. The temperature T_{COK} also shows the crossover for nucleation of kink rings with no attached vortices, and $T_{\text{COK}} = 0$ with the zero Josephson coupling strength $q = 0$ because there is no energy cost for kinks to be nucleated. We note that overall behaviors shown in Figs 2 (a), (b), and 3 (c) are qualitatively unchanged among different imbalanced densities $n_1/n_2 \neq 1$.

Figure 4 shows equilibrium snapshots of vortices and kinks. At $T = T_{\text{COV}}$, there are vortex-antivortex pairs for the first component connected with kinks as shown in (a). At $T = T_{\text{BKT}}$, there are not only vortex-antivortex pairs for both components but also molecule-antimolecule pairs denoted by green dashed closed lines. In both (a) and (b), we can see kink rings with no attaching vortices which start to frequently appear at T_{COK} .

For the balanced density $n_1 = n_2$ shown in Fig. 3 (b), two number densities $\rho_{v1} \simeq \rho_{v2}$ and the length density ρ_k deviate from the Arrhenius relation at the BKT transition temperature $T_{\text{BKT}} (= T_{\text{COV}})$ and the crossover temperature T_{COK} , respectively.

In conclusion, we have investigated the two-dimensional Bose system with two quantum sublevels. The phases of both components can be coupled through the Josephson oscillation. When the Josephson coupling is absent, topologically stable fractional vortices induce two-step BKT transitions having the normal universal

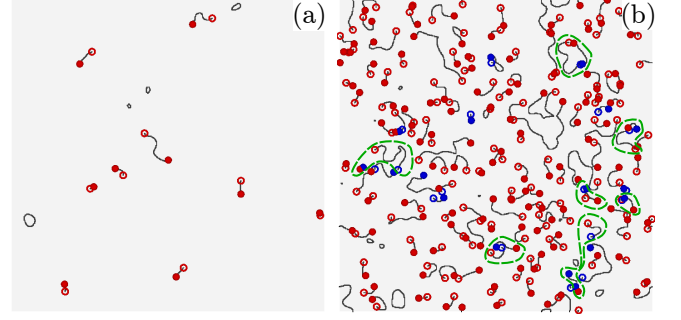


FIG. 4. Equilibrium snapshots of vortices and kinks with $L = 64\xi$, $n_1/n_2 = 0.5$ and $q = 0.1gn$ at (a): $T = T_{\text{COV}}$ and (b): $T = T_{\text{BKT}}$. Closed (open) red and blue circles represent positions of vortices for $\{1, 0\}$ and $\{0, 1\}$ ($\{-1, 0\}$ and $\{0, -1\}$) respectively. Black solid lines show kinks. Green dashed closed lines in panel (b) denote molecule-antimolecule pairs.

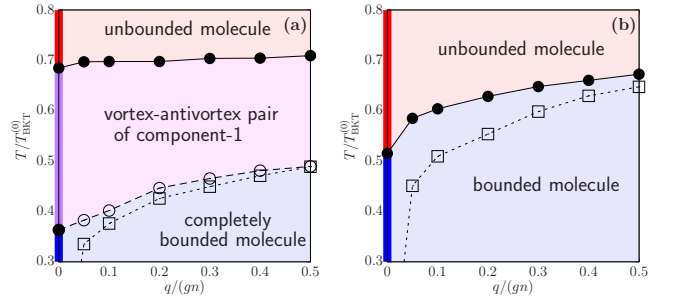


FIG. 5. Phase diagrams for the temperature T and the Josephson coupling q for (a): $n_1/n_2 = 0.5$ and (b): $n_1/n_2 = 1$. The red, purple, and blue lines at $q = 0$ show phases for unbounded vortex of both components, unbounded vortex of the first component, and bounded vortex of both component, respectively. The black solid lines and filled circles show the BKT transition temperature T_{BKT} . The dashed line with open circles in panel (a) and dotted lines with open squares in the both panels indicate the crossover temperatures T_{COV} and T_{COK} .

relation in Eq. (1), which suggests that the fractional circulation does not affect the universal relation in contrast to the conventional understanding. This result is qualitatively independent of the value of the inter-component interaction strength g_2 . When the Josephson coupling is switched on, the BKT transition occurs once for both balanced and imbalanced densities, and the universal relation is unchanged even for the balanced density. This result can be understood from the interaction between vortices as shown in Eq. (7). There are additional linear interactions between a vortex and its antivortex in Eqs. (7b) and (7c) which hinder the BKT transition by binding of them. Instead of single-component vortex pairs, molecule-antimolecule pairs having pure logarithmic interactions in Eq. (7d) induces the BKT transition of this system. For the case of imbalanced densities,

however, there is a characteristic temperature T_{COV} at which single-component vortex-antivortex pairs start to form bound states as a relic of the BKT transition without the Josephson coupling. The temperature T_{COV} does thermodynamically not give the transition but gives the crossover. We also find a lower crossover temperature T_{COK} than T_{COV} at which kink rings with no attaching vortices start to be nucleated. We summarize our discussion with the phase diagrams shown in Fig. 5.

ACKNOWLEDGEMENT

We would like to thank Yuki Kawaguchi and Atsutaka Maeda for the helpful suggestions and comments. This work is supported by the Japan Society for the Promotion of Science (JSPS) Grant-in-Aid for Scientific Research (KAKENHI Grant No. 16H03984). The work is also supported in part by Grant-in-Aid for Scientific Research (KAKENHI Grant Numbers 26870295 (MK), 16KT0127 (MK), 26800119 (ME) and 17H06462 (ME)). The work of MN is supported in part by the Ministry of Education, Culture, Sports, Science (MEXT)-Supported Program for the Strategic Research Foundation at Private Universities “Topological Science” (Grant No. S1511006), and by a Grant-in-Aid for Scientific Research on Innovative Areas “Topological Materials Science” (KAKENHI Grant No. 15H05855) from the the Ministry of Education, Culture, Sports, Science (MEXT) of Japan.

-
- [1] V. L. Berezinski, Sov. Phys. JETP, **32**, 493 (1971).
 [2] J. M. Kosterlitz and D. J. Thouless, J. Phys. C, **6**, 1181 (1973).
 [3] S. Coleman, Commun. math. Phys. **31**, 259 (1973).
 [4] N. D. Mermin and H. Wagner, Phys. Rev. Lett. **17**, 1133 (1966).
 [5] P. C. Hohenberg, Phys. Rev. **158**, 383 (1967).
 [6] D. J. Bishop and J. D. Reppy, Phys. Rev. Lett. **40**, 1727 (1978).
 [7] D. U. Guster and S. A. Wolf, Solid State Comm. **32**, 449 (1979).
 [8] A. F. Hebard and A. T. Fiory, Phys. Rev. Lett. **44**, 291 (1980).
 [9] R. F. Voss, C. M. Knoedler, and P. M. Horn, Phys. Rev. Lett. **45**, 1523 (1980).
 [10] S. A. Wolf, D. U. Gubser, W. W. Fuller, J. C. Garland, and R. S. Newrock, Phys. Rev. Lett. **47**, 1071 (1981).
 [11] K. Epstein, A. M. Goldman, and A. M. Kadin, Phys. Rev. Lett. **47**, 534 (1981).
 [12] D. J. Resnick, J. C. Garland, J. T. Boyd, S. Shoemaker, and R. S. Newrock, Phys. Rev. Lett. **47**, 1542 (1981).
 [13] R. F. Voss and R. A. Webb, Phys. Rev. B **25**, 3446 (1982).
 [14] B. I. Halperin and D. R. Nelson, Phys. Rev. Lett. **41**, 121 (1978).
 [15] A. P. Young, Phys. Rev. B **19**, 1885 (1979).
 [16] K. Zahn, R. Lenke, and G. Maret, Phys. Rev. Lett. **82**, 2721 (1999);
 [17] Z. Hadzibabic, P. Krüger, Marc Cheneau, B. Battelier, and J. Dalibard, Nature **441**, 1118 (2006).
 [18] M. M. Salomaa and G. E. Volovik, Phys. Rev. Lett. **55**, 1184 (1985); Rev. Mod. Phys. **59**, 533 (1987).
 [19] G. E. Volovik, *The Universe in a Helium Droplet* (Clarendon Press, Oxford, 2003).
 [20] S. Autti, V. V. Dmitriev, J. T. Mäkinen, A. A. Soldatov, G. E. Volovik, A. N. Yudin, V. V. Zavjalov, and V. B. Eltsov, Phys. Rev. Lett. **117**, 255301 (2016).
 [21] D. A. Ivanov, Phys. Rev. Lett. **86**, 268 (2001).
 [22] S. B. Chung, H. Bluhm, and E.-A. Kim, Phys. Rev. Lett. **99**, 197002 (2007); S. B. Chung and S. A. Kivelson, Phys. Rev. B **82**, 214512 (2010).
 [23] J. Jang, D. G. Ferguson, V. Vakaryuk, R. Budakian, S. B. Chung, P. M. Goldbart, and Y. Maeno, Science **331**, 186 (2011).
 [24] E. Babaev, Phys. Rev. Lett. **89**, 067001 (2002); E. Babaev, A. Sudbo, and N. W. Ashcroft, Nature (London) **431**, 666 (2004); J. Smiseth, E. Smorgrav, E. Babaev, and A. Sudbo, Phys. Rev. B **71**, 214509 (2005); E. Babaev and N. W. Ashcroft, Nat. Phys. **3**, 530 (2007).
 [25] J. Goryo S. Soma, and H. Matsukawa, Europhys. Lett. **80**, 17002 (2007).
 [26] A. Crisan *et al.*, T. Watanabe, Jpn. J. Appl. Phys. **46**, L451-L453 (2007); Y. Tanaka *et al.*, Jpn. J. Appl. Phys. **46**, 134-145 (2007); A. Crisan *et al.*, K. Tokiwa, T. Watanabe, T. W. Button, and J. S. Abell, Phys. Rev. B **77**, 144518 (2008); J. W. Guikema *et al.*, Phys. Rev. B **77**, 104515 (2008); L. Luan *et al.*, Phys. Rev. B **79**, 214530 (2009).
 [27] Y. Tanaka, H. Yamamori, T. Yanagisawa, T. Nishio, S. Arisaw, Physica C (in press).
 [28] T.-L. Ho, Phys. Rev. Lett. **81**, 742 (1998); T. Ohmi and K. Machida, J. Phys. Soc. Jpn. **67**, 1822 (1998).
 [29] G. W. Semenoff and F. Zhou, Phys. Rev. Lett. **98**, 100401 (2007); M. Kobayashi, Y. Kawaguchi, M. Nitta, and M. Ueda, Phys. Rev. Lett. **103**, 115301 (2009); J. Huhtamäki, T. Simula, M. Kobayashi, and K. Machida, Phys. Rev. A **80**, 051601 (2009).
 [30] D. T. Son and M. A. Stephanov, Phys. Rev. A **65**, 063621 (2002).
 [31] E. J. Mueller and T.-L. Ho, Phys. Rev. Lett. **88**, 180403 (2002).
 [32] K. Kasamatsu, M. Tsubota, and M. Ueda, Phys. Rev. Lett. **91**, 150406 (2003).
 [33] K. Kasamatsu, M. Tsubota, and M. Ueda, Int. J. Mod. Phys. B **19**, 1835 (2005).
 [34] A. Aftalion, P. Mason, and J. Wei, Phys. Rev. A **85**, 033614 (2012).
 [35] P. Kuopanportti, J. A. M. Huhtamäki, and M. Möttönen, Phys. Rev. A **85**, 043613 (2012).
 [36] K. Kasamatsu, M. Tsubota, and M. Ueda, Phys. Rev. Lett. **93**, 250406 (2004).

- [37] K. Kasamatsu and M. Tsubota, Phys. Rev. A **79**, 023606 (2009).
- [38] M. Eto, K. Kasamatsu, M. Nitta, H. Takeuchi and M. Tsubota, Phys. Rev. A **83**, 063603 (2011).
- [39] M. Eto and M. Nitta, Phys. Rev. A **85**, 053645 (2012).
- [40] M. Eto and M. Nitta, EPL **103**, no. 6, 60006 (2013).
- [41] M. Cipriani and M. Nitta, Phys. Rev. Lett. **111**, 170401 (2013).
- [42] M. Cipriani and M. Nitta, Phys. Rev. A **88**, 013634 (2013).
- [43] D. S. Dantas, A. R. P. Lima, A. Chaves, C. A. S. Almeida, G. A. Farias and M. V. Miloevi, Phys. Rev. A **91**, 023630 (2015).
- [44] K. Kasamatsu, M. Eto and M. Nitta, Phys. Rev. A **93**, no. 1, 013615 (2016).
- [45] M. Tylutki, L. P. Pitaevskii, A. Recati and S. Stringari, Phys. Rev. A **93**, no. 4, 043623 (2016).
- [46] M. Eto and M. Nitta, Phys. Rev. A **97**, no. 2, 023613 (2018).
- [47] B. M. Uranga and A. Lamacraft, arXiv:1801.09912 [cond-mat.quant-gas]
- [48] Y. G. Rubo, Phys. Rev. Lett. **99**, 106401 (2007); K. G. Lagoudakis, T. Ostatnický, A. V. Kavokin, Y. G. Rubo, R. Andre, and B. Deveaud-Pledran, Science **326**, 974 (2009); Y. G. Rubo, arXiv:1209.6538; G. Roumpos, M. D. Fraser, A. Löffler, S. Höfling, A. Forchel, and Y. Yamamoto, Nat. Phys. **7**, 129 (2011).
- [49] J. Keeling and N. G. Berloff, Phys. Rev. Lett. **100**, 250401 (2008); M. O. Borgh, G. Franchetti, J. Keeling, and N. G. Berloff, Phys. Rev. B **86**, 035307 (2012).
- [50] L. M. Pismen, Phys. Rev. Lett. **72**, 2557 (1994); L. M. Pismen, Physica (Amsterdam) D **73**, 244 (1994); I. S. Aranson and L. M. Pismen, Phys. Rev. Lett. **84**, 634 (2000); L. M. Pismen, *Vortices in Nonlinear Fields: From Liquid Crystals to Superfluids, from Non-Equilibrium Patterns to Cosmic Strings* (Oxford University Press, New York, 1999).
- [51] A. P. Balachandran, S. Digal, and T. Matsuura, Phys. Rev. D **73**, 074009 (2006); E. Nakano, M. Nitta, and T. Matsuura, Phys. Rev. D **78**, 045002 (2008); M. Eto and M. Nitta, Phys. Rev. D **80**, 125007 (2009); M. Eto, E. Nakano, and M. Nitta, Phys. Rev. D **80**, 125011 (2009); M. Eto, M. Nitta, and N. Yamamoto, Phys. Rev. Lett. **104**, 161601 (2010); M. Eto, Y. Hirono, M. Nitta and S. Yasui, PTEP **2014**, no. 1, 012D01 (2014).
- [52] D. L. Stein and M. C. Cross, Phys. Rev. Lett. **42**, 504 (1979).
- [53] S. E. Korshunov, Zh. Eksp. Teor. Fiz. **89**, 531 (1984).
- [54] Y. Tanaka, J. Phys. Soc. Jp. **70** (2001) 2844; Phys. Rev. Lett. **88** (2001) 017002.
- [55] S. Mukerjee, C. Xu, and J. E. Moore, Phys. Rev. Lett. **97**, 120406 (2006).
- [56] A. J. A. James and A. Lamacraft, Phys. Rev. Lett. **106**, 140402 (2011).
- [57] A. Y. Liu, I. I. Mazin, and J. Kortus, Phys. Rev. Lett. **87**, 087005 (2001).
- [58] A. Brinkman, A. A. Golubov, H. Rogalla, O. V. Dolgov, J. Kortus, Y. Kong, O. Jepsen, and O. K. Andersen, Phys. Rev. B **65** 180517 (2002).
- [59] A. A. Golubov, J. Kortus, O. V. Dolgov, O. Jepsen, Y. Kong, O. K. Andersen, B. J. Gibson, K. Ahn, and R. K. Kremer, J. Phys.: Condens. Matter **14**, 1353 (2002).
- [60] H. J. Choi, D. Roundy, H. Sun, M. L. Cohen, and S. G. Louie, Phys. Rev. B **66** 020513 (2002).
- [61] Y. Kamihara, T. Watanabe, M. Hirano, and H. Hosono, J. Am. Chem. Soc. **130**, 3296 (2008).
- [62] D. J. Singh and M.-H. Du, Phys. Rev. Lett. **100**, 237003 (2008).
- [63] I. I. Mazin, D. J. Singh, M. D. Johannes, and M. H. Du, Phys. Rev. Lett. **101**, 057003 (2008).

Appendix A: Fixing BKT critical temperatures

The Binder ratio

$$b \equiv 1 - \frac{\langle \{ |\Psi_1|^2 + |\Psi_2|^2 \}^2 \rangle}{3 \langle |\Psi_1|^2 + |\Psi_2|^2 \rangle^2}, \quad (\text{A1})$$

becomes size independent for the critical states below the BKT transition temperature. Here, Ψ_i is defined as

$$\Psi_i \equiv \frac{1}{L^2} \int d^2x \psi_i. \quad (\text{A2})$$

Figure 6 shows two typical examples of the Binder ratio

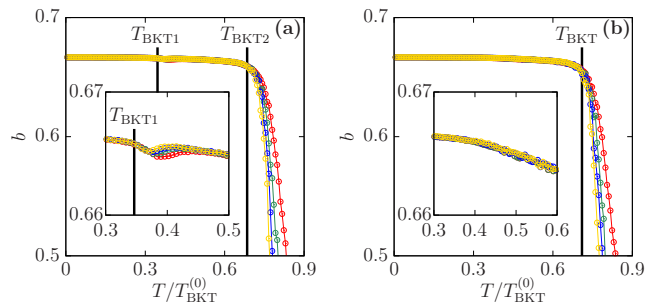


FIG. 6. Binder ratio b for $n_1/n_2 = 0.5$ and system sizes $L_1 = 64\xi$ (red lines), $L_2 = 96\xi$ (green lines), $L_3 = 128\xi$ (blue lines), and $L_4 = 160\xi$ (yellow lines). The Rabi coupling strength is fixed as (a) $q = 0$ and (b) $q = 0.1gn$. The BKT transition temperatures (T_{BKT1} and T_{BKT2} in panel (a) and T_{BKT} in panel (b)) are shown as solid lines. In insets for both panels, we zoom over temperatures around $T = 0.4T_{\text{BKT}}^{(0)}$.

b with the Rabi coupling strength $q = 0$ and $q = 0.1gn$ for the imbalanced density $n_1/n_2 = 0.5$. With four different system sizes, the BKT transition temperature is estimated as the temperature at which four Binder ratios start to differ:

$$\frac{1}{4\bar{b}} \sqrt{\sum_{i=1}^4 (b(L_i) - \bar{b})^2} \lesssim 0.01, \quad \bar{b} \equiv \frac{1}{4} \sum_{i=1}^4 b(L_i). \quad (\text{A3})$$

For the zero Rabi coupling strength $q = 0$ shown in Fig. 6 (a), there are two transition temperatures $T_{\text{BKT1}} \simeq 0.36T_{\text{BKT}}^{(0)}$ and $T_{\text{BKT2}} \simeq 0.68T_{\text{BKT}}^{(0)}$ for the first (see the inset in Fig. 6 (a)) and second components, respectively. For the nonzero Rabi coupling strength $q = 0.1gn$ in Fig.

6 (b), on the other hand, the BKT transition at the low temperature around $T \sim 0.35T_{\text{BKT}}^{(0)}$ disappears and occurs only once at the temperature $T_{\text{BKT}} \simeq 0.71T_{\text{BKT}}^{(0)}$. All other BKT transition temperatures T_{BKT} in the manuscript are obtained by the same way.

Obtained BKT transition temperatures can be also justified by the correlation function

$$C(r) = \frac{1}{nL^2} \sum_{i=1}^2 \int d^2x \int \frac{d\Omega_{\mathbf{r}}}{2\pi r} \langle \psi_i^*(\mathbf{x}) \psi_i(\mathbf{x} + \mathbf{r}) \rangle, \quad (\text{A4})$$

where $\Omega_{\mathbf{r}}$ is the solid angle for the vector \mathbf{r} . In the thermodynamic limit $L \rightarrow \infty$, the correlation function $C(r)$ show the algebraic decrease $C(r) \propto r^{-\eta(T)}$ with the temperature-dependent critical exponent $\eta(T)$ at low temperatures $T \leq T_{\text{BKT}}$. The correlation func-

tion $C(r)/L^{-\eta}$ is expected to be a universal function on r/L below BKT critical temperatures. We can see this universality in Fig. 7 with $\eta = 1/4$ at $T = T_{\text{BKT2}}$ (panel (a)) and $T = T_{\text{BKT}}$ (panels (b-d)). The value of the exponent $\eta = 1/4$ is same as that for the single-component Bose gas at the BKT critical temperature. Our results in Fig. 7 support the correctnesses of our estimations for the BKT critical temperatures and suggest that the critical exponent is unchanged between the single-component and multi-component Bose gases.

Considering the universality at $T = T_{\text{BKT1}}$ for the imbalanced density $n_1/n_2 \neq 1$ and the zero Josephson coupling strength $q = 0$, we should use the correlation function $C_1(r)$ for the 1st component defined as

$$C_1(r) = \frac{1}{n_1 L^2} \int d^2x \int \frac{d\Omega_{\mathbf{r}}}{2\pi r} \langle \psi_1^*(\mathbf{x}) \psi_1(\mathbf{x} + \mathbf{r}) \rangle, \quad (\text{A5})$$

instead of the global correlation function $C(r)$. In the same way as $C_1(r)$, we can define $C_2(r)$ for the second component and its exponent is smaller than $1/4$ because the BKT transition for the second component occurs at the higher temperature $T_{\text{BKT2}} > T_{\text{BKT1}}$. The universal-

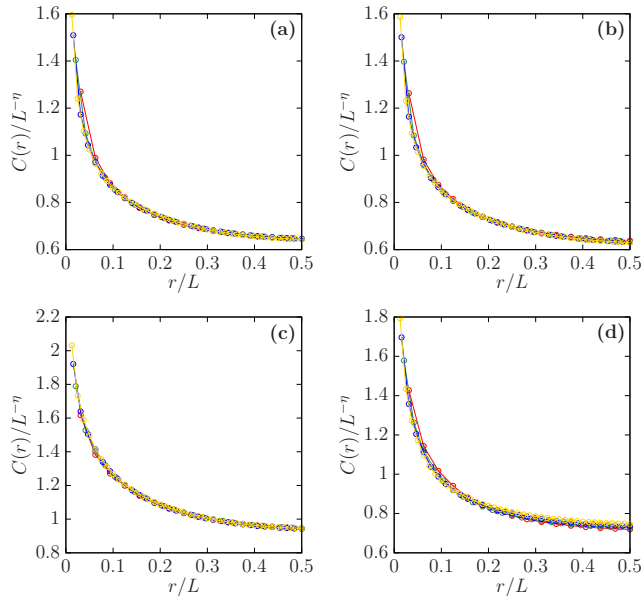


FIG. 7. Finite-size scaling of the correlation function $C(r)$ for (a) $n_1/n_2 = 0.5$ and $q = 0$, (b) $n_1/n_2 = 0.5$ and $q = 0.1gn$, (c) $n_1/n_2 = 1$ and $q = 0$, and (d) $n_1/n_2 = 1$ and $q = 0.1gn$ at the BKT transition temperature (a) $T = T_{\text{BKT2}}$ and (b-d) $T = T_{\text{BKT}}$. The critical exponent is fixed as $\eta = 1/4$. For the system size, we use the same colors as those in Fig. 6.

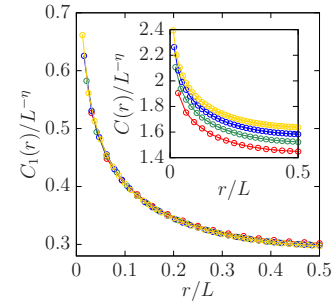


FIG. 8. Finite-size scaling of the correlation function $C_1(r)$ for $n_1/n_2 = 0.5$ and $q = 0$ at the BKT transition temperature $T = T_{\text{BKT1}}$. The critical exponent is fixed as $\eta = 1/4$. For the system size, we use the same colors as those in Fig. 6. Inset: Finite-size scaling of the correlation function $C(r)$.

ity of $C_1(r)$ with $\eta = 1/4$ at $T = T_{\text{BKT}}$ can be confirmed as shown in Fig. 8, whereas $C(r)$ fails to satisfy the universal property as shown in the inset of Fig. 8.